# High-Efficiency Sub-Micrometer Multi-Beam Interference Structuring for Large-Scale Surface Using Ultrashort Laser Pulses

Chao He*, Kai Vannahme** and Arnold Gillner*,**

*Chair for Laser Technology LLT, RWTH Aachen University, Steinbachstrasse 15, 52074 Aachen, Germany
**Fraunhofer Institute for Laser Technology ILT, Steinbachstrasse 15, 52074 Aachen, Germany
E-mail: chao.he@llt.rwth-aachen.de

Laser direct structuring using multi-beam interference can fabricate one and two-dimensional periodic patterns with a structural periodicity from hundred nanometer to tens of micrometer. Nevertheless, the structuring efficiency, which is relative to patterning speed, structure periodicity, depth and laser fluence applied, and homogeneity of interference pattern are still the main concerns and need to be taken into consideration especially for large-scale surface. In this paper, the structuring efficiency of two beam interference was defined and was investigated on tool steel using an ultrashort pulsed (USP) laser. During the multi-beam interference structuring, the USP laser, which has a pulse width of 10 picoseconds, worked at a wavelength of 532 nm and repetition rate of 100 kHz. Linear patterns with a periodicity of 940 nm and was fabricated on an area of 100 mm × 100 mm. We achieved a patterning speed up to 500 mm/s on the surface of tool steel by means of an x-y linear working stage. The local morphology was analyzed by an atom force microscopy (AFM). Moreover, the global homogeneity of the patterned surface was quantitatively characterized. The results demonstrated a stable structuring process with minor deviation of structure periodicity and depth.
DOI: 10.2961/jlmn.2019.01.0016
**Keywords:** multi-beam interference, ultrashort pulsed laser, large-scale surface structuring, sub-micrometer, periodic structures

## 1. Introduction

The fabrication of periodic micro and nanostructures by direct laser irradiation has been intensively studied in recent decades. Bringing such structures onto the surface of modern devices have the potentials to generate new functions or to enhance their mechanic, optical or biological performance [1-4]. One effective approach to create periodic nanostructures on a large area is to apply ultrashort pulsed (USP) laser irradiation especially in regime of femtosecond. Laser induced high frequency ripples and laser induced periodic surface structures (LIPSS) can achieve structures with periodicities in the same magnitude of or even significantly shorter than laser wavelength on a variety of materials[5-8]. The interesting phenomenon has aroused great attentions of researchers. Huang, et. al. obtained nanostructures on graphite with multi-periodicities about 200 nm and 120 nm by irradiation of a 800 nm wavelength fs laser. An area of 200 μm×200 μm was structured with an effective scanning speed of 1 m/s[9]. Harzic et. al. generated high-spatial-frequency patterns of λ/6 periodicity (115-151 nm) by a nanojoule-femtosecond laser scanning technique on a 10 $mm^2$ silicon area. The scanning speed was 1 mm/s [10]. Schiller et.al used a high pulse repetition frequency femtosecond laser and a fast galvanometer scanner system to process zirconium oxide (size 80 × 80 $mm^2$). Ripple formation with a periodicity of approximately 900 nm can be observed. A processing rate of 25 $cm^2$/min was achieved [11].

However, the requirement on productivity in industrial applications especially those with large scale surface becomes ever higher. High throughput together with high precision is the aim of micro and nanostructuring for macro parts. However, the limitation of process speed is dependent on laser performance like available laser pulse energy, coherent length, as well as ablation threshold of materials. Thanks to the rapid development of laser source, especially the ultrashort pulsed laser sources, a KW-class USP laser is now available on the market [12].

As a laser direct ablation process, multi-beam interference (MBI) patterning enables the precise fabrication of structures with periodicity from sub-micrometer to several micrometer[13, 14]. With the advantage of tuning the structural periodicity and minimization of thermal effect, multi-beam interference with ultrashort laser pulses has been demonstrated to be a more effective and flexible microstructuring technique. The microstructure with the combination of LIPSS and interference pattern was published in 2010 by Nakata et. al.[15] They used a 2D-FFT is useful to analyze the periodicity of obscure structures. Lasagni et al.[16-18] achieved a structuring speed of about 0.1 $m^2$/min with spatial periodicity ranging from 2.2 to 3.1 μm in metals using a galvanometric scanner and a nanosecond laser source. The pattern on stainless steel with 1 μm period had a structure depth of only approximately 35 nm. Recently, they employed ps-laser sources to fabricate periodic surface patterns on Ni-sleeves and achieved a speed of 57 $cm^2$/min [19]. The microstructure is a combination of multi-beam interference pattern with a periodicity of 0.5 -20 μm (low frequency) and LIPSS with a periodicity of 0.2 μm(high frequency). The ablation depth is below a couple of hundred nanometers.

Our previous works have been aimed to achieve a higher resolution in fabricating periodic nanostructures using multi-beam interference [20-22]. The patterning speed has a lower order of priority compared with structural quality. Nevertheless, many works have also been done in order to accelerate the structuring process. An approach was adopted by using consecutively deposited laser pulse. As a part of a following research project, the focus of this work lies on the enhancement of structuring efficiency for large-scale surface by using a position synchronized output. Meanwhile, the resolution and local homogeneity regarding the depth and the periodicity of the sub-micron structures will be analyzed by a two dimensional fast Fourier transform (2D FFT).

## 2. Experimental setup

### 2.1 System for USP laser multi-beam interference

Fig. 1 shows the experimental setup of the multi-beam interference for fabrication of periodic nanostructure. A diode pumped Nd:$YVO_4$ Innoslab laser (PX100 Series, EdgeWave), which emits a 532 nm wavelength irradiation, is applied as the laser beam source. The laser pulse duration is 10 ps and maximum energy 185 µJ at a working repetition rate of 100 kHz. In this work, the laser single pulse energy was fixed at the maximum 185 µJ due to the consideration of a relative high ablation threshold of the material and to scale up the structuring efficiency. The incident beam is firstly focused by an $f$=500 mm aspheric focusing lens and then split by a diffractive optical element (DOE). The DOE splits the incident laser beam in one dimension and designed for the enhancement of the power distribution in $\pm1^{st}$ orders, which contain approximately 80% of the total incident laser power. Apart from the $\pm1^{st}$ orders, the $0^{th}$ order, which cannot be eliminated, and all other higher orders of the laser beam are blocked by a filter. The two coherent beams ($\pm1^{st}$ order) are symmetrically reflected by a high-reflection coated knife-edge prism to two tunable mirrors, whose rotation angle can be tuned and thus the incident angle of two laser beams on the sample can be adjusted. In this work, the incident angle $\alpha$ was adjusted to 16°. The scanning direction is in consistence with the orientation of the interference pattern. A 100 mm×100 mm tool steel X40Cr14 with a maximum hardness of 55 HRC (Rockwell C hardness) was used as sample and placed on a XY axis system (Planar DL-100, Aerotech). The surface roughness of the sample is $R_a$=30 nm.

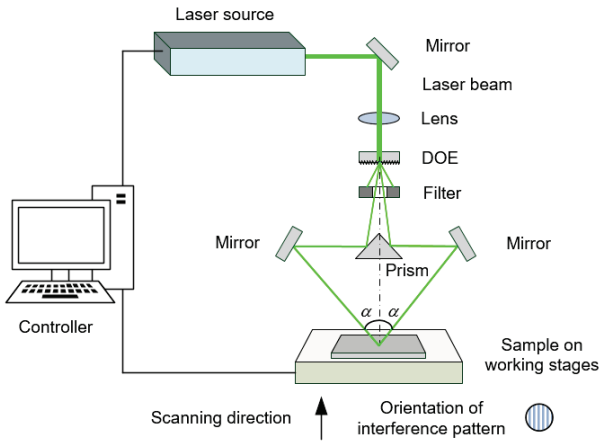


**Fig. 1** Schematic diagram of the experimental setup for the multi-beam interference (MBI)

### 2.2 Triggering with a Position Synchronized Output (PSO)

The axis system is capable of achieving a maximum velocities of 500 mm/s and a straightness down to ± 0.4 µm. The core of the technique of this work is the Position Synchronized Output (PSO). The PSO is a subsystem of the axis system that works as a trigger for the laser and enables a submicrometer accuracy of laser spot placement especially at high acceleration. The laser output is tightly connected with the position of axis, so that the temporary pulse deposition is not synchronized with the fixed pulse repetition rate but the position of pulses. In other words, the PSO works as a process trigger tool based on distance traveled, avoiding trigger errors based on acceleration, deceleration, or any other velocity instability. The triggering principle with and without a PSO is compared and depicted in Fig. 2. In PSO mode, the laser is triggered on with a fire command each time the axis has moved the specified distance of $\delta$. In the time domain, the pulses triggered on (PSO output) are determined by the actual distance traveled, instead of the independence on the fixed pulse repetition rate in non-PSO mode, For the laser multi-beam interference, the distance between spots (pulse position) and the number of pulses on each position can be controlled by the fire command. In this work, the distance is varied from 75 µm to 175 µm, and number of pulses from 1 to 3 pulses. With the PSO output the patterning is a process with consecutively deposited laser pulse. The axis moves non-stop during the triggering of laser pulses.

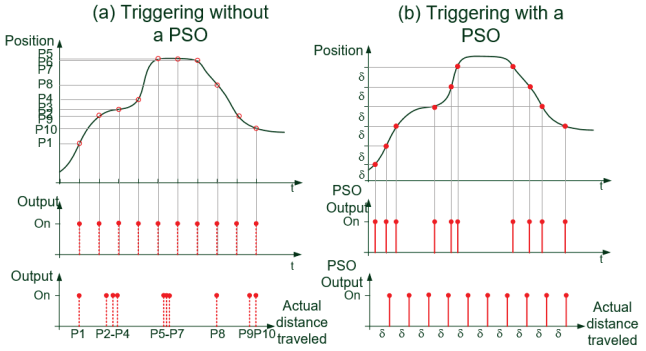


**Fig. 2** Pulse triggering without (a) and with (b) a Position Synchronized Output(PSO)

### 2.3 Structural characterization

The morphology of irradiated samples was analyzed by means of an atomic force microscope (AFM, Rados N8, Bruker).The experiments were conducted with a laser spot size of 180 µm on the sample surface. First of all, the structuring speed, pulse numbers at each position and distance between spots and paths were varied for the purpose of identification of optimized parameter windows for a high quality structuring. To characterize the stability of patterned microstructure under different processing conditions the scanning speed is varied from 200 mm/s to 480 mm/s with a 40 mm/s pitch. The periodicity of the patterned structures is investigated by 2D FFT analysis.

## 3. Results and discussion

### 3.1 Pulse overlap

In the laser ablation process, the pulse overlap $\eta_p$ can be give as following according to [23]:

$$\eta_p = 1 - \frac{(\tau_p + 1/f) \cdot v_s}{2\omega_0} \quad (1)$$

Here, $\tau_p$ is single pulse duration, $f$ repetition rate of laser pulses, $v_s$ is the scanning speed or the feed rate of the motion axis, and $\omega_0$ is radius of laser spot at focal plane of laser beam. Since the pulse duration $\tau_p$=10 ps($10\times10^{-12}$ s), << $1/f$= $1\times10^{-5}$ s, thus the equation 1 can be simplified as:

$$\eta_p = 1 - \frac{v_s}{2\omega_0 \cdot f} \quad (2)$$

Since the patterning speed is about 500 mm/s and the patterning length of one path is 100 mm, an acceleration and deceleration of axis motion must be taken into consideration. Thus, the pulse overlap is not constant and influenced by an acceleration/deceleration process. This process can be described as the differential of scanning speed in time domain $dv_s/dt$. Whereas the evolution of pulse overlap over time can be given as:

$$\frac{d\eta_p}{dt} = -\frac{1}{2\omega_0 \cdot f} \cdot \frac{dv_s}{dt} \quad (3)$$

From the equation 3, the pulse overlap is inconstant when an acceleration or deceleration occurs during the triggering without a PSO. The pulse density at unit length varies which leads to an inhomogeneous energy deposition on the path. As a result, the homogeneity of ablation depth on the path is undermined and possible locally overloaded thermal effect is induced. By taking advantage of the PSO output, the distance between the neighbored pulses and the pulse number at each positon can theoretically remain to be constant in case of acceleration or deceleration. Rephrased, the overlapping degree and pulse density on the structuring path can be kept as a constant. The duty cycle of the laser output with PSO $DC_{PSO}$ is given by:

$$DC_{PSO} = \frac{1/f}{\delta/v_s} \cdot \quad (4)$$

With a pulse distance of 75 µm and scanning speed of 500 mm/s, the trigger interval of PSO is calculated to be 150 µs, which is 15 times of the pulse repetition interval 10 µs ($f$=100 kHz). The duty cycle of the laser output with PSO is approximately 6.7%.

### 3.2 Influence of processing parameters

Fig. 3 shows the macro optical image of the patterned surface irradiated by varied parameters including the structuring speed, pulse number and distance between laser spots and neighbored paths. Among that, the number of pulses as well as the distance between spots are two key factors for the energy deposition of laser pulses at each position. The number of pulses describes the total fluence applied at each position for the patterning. While the distance between spots and paths determines the overlap degree of neighbored laser spots and spatial pulse energy deposition as well as heat accumulation. With the increase of pulse number, the patterned area becomes darker, it indicates a stronger ablation. The similar phenomenon occurs when the neighbored pulses locate closer to each other. Worthy to be noted is that, with the same pulse number and spots distance for example 3 pulses at each position and 150 µm pitch between neighbored spots, the patterned areas show the same optical appearance and is independent on the structuring speed.

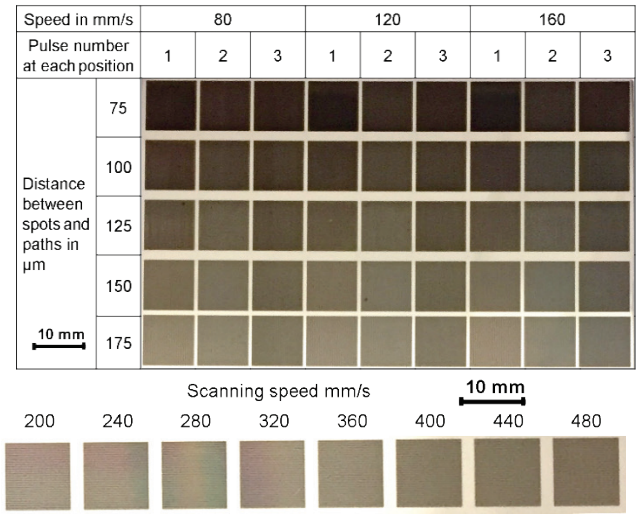


**Fig. 3** Optical images of patterned surface using MBI. The size of each square is 10 mm×10 mm, single pulse energy 185 µJ, repetition rate, 100 kHz, two pulse at each position.

By taking the optical surface quality regarding the degree of diffraction effect and thermal effect as a criteria, the pulse number of 2 and the distance of 175 µm between spots were selected and applied as the optimal parameters for further investigation on varied higher structuring speeds. The macro optical appearance with varied scanning speed is shown in Fig. 3.

### 3.3 Characterization of patterned structures

The macro optical appearance provides insufficient details on the morphology of the patterned structures. To characterize the stability of patterning with different structuring speeds, the samples were analyzes under an atomic force microscope (AFM). The AFM images show the local morphology of the patterns in an area of 10 by 10 µm$^2$. Nine periods of the single lines were included and measured to get an average value of depth and minimize the deviation. By means of an analytic software, the profile of sub-micrometer structures on the sample with scanning speed of 280 mm/s from Fig. 3 were extracted and calculated as shown in Fig. 4. The average depth and the periodicity of linear structures are measured. The average periodicity was measured to be 940 nm and an average depth of 245 nm. The aspect ratio of the patterned structure is more than 1:4.

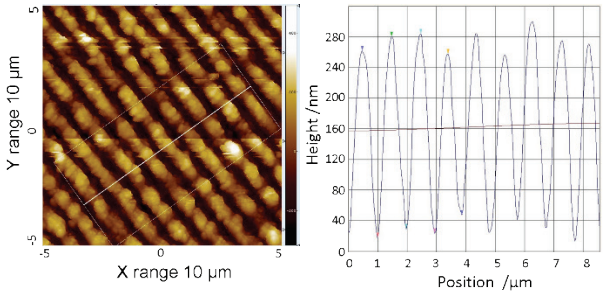


**Fig. 4** Measurement of structural profile for characterization of patterning stability from Fig. 3. Structuring speed 280 mm/s, single pulse energy 185 µJ, repetition rate 100 kHz

The AFM analyze on the morphology of samples structured in micro scale under varied patterning speed is shown in Fig. 5. No significate difference regarding periodicity can be noticed from the surface morphology. The positions of the

measured area is carefully selected so that the depth of structure by different patterning speeds is comparable Since the global homogeneity of the periodic structures between the different shots is studied in our previous work [16], the center of the laser spot is chosen in this work. The patterns fabricated with relative slow speeds (240 and 280 mm/s) as well as faster speeds (400 and 480 mm/s) show well-defined linear periodic structures and good contrast. By using a 2D FFT analysis, the periodicity of patterned structures is investigated and shown in Fig. 5(e), the peaks of the curves lie at the x position between 1.06±0.01 μm$^{-1}$ in the frequency-domain, which indicates that the structures have a constant spatial frequency and the periodicity of the patterned structures with varied scanning speed is stable.

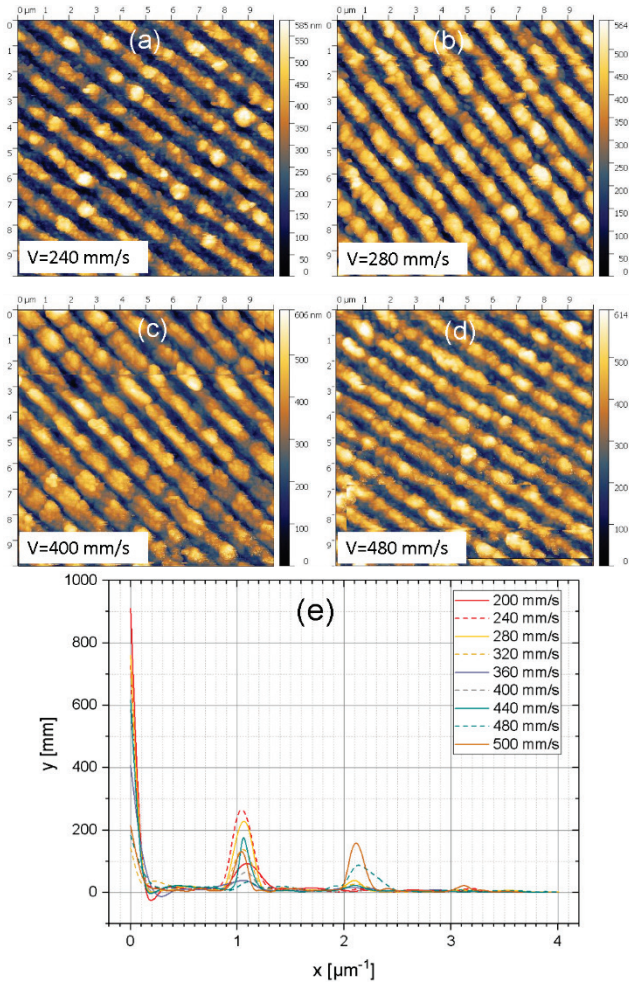


**Fig. 5** (a-d): AFM images of MBI patterns with varied scanning speeds, (e): 2D FFT analysis on the periodicity of patterned structures. Laser parameter: single pulse energy 185 μJ, repetition rate 100 kHz

The average depth of patterns are plotted over structuring speed as shown in Fig. 6. From the plotted diagram, despite that a slight fluctuation is present, the average depth values remain in a small range around 250±20 nm. The deviation can be caused by e. g. wear of the AFM tip or positioning error. A linear fit of all the depth values shows a very gentle incline, which gives an evidence that the patterned structures by multi-beam interference with an up-scaled velocity is comparable to those with relative lower ones. This is due to a constant pulse deposition in the structuring process. With a specified pulse number and spots distance, that controlled by the PSO system, the position of pulse deposition is independent on the scanning speed. It contributes to a constant pulse overlap on the structure path. Moreover, the laser fluence applied is consistent under different scanning speeds, therefore the ablation depth stays in the same magnitude, whereas the patterning efficiency is enhanced with a factor of at least 2.5 in this case. According to equation 2, there is a slight different between the overlap of the sequential pulses at each position under different scanning velocities, the fluctuation is ascribable to this difference of inter-pulse overlap.

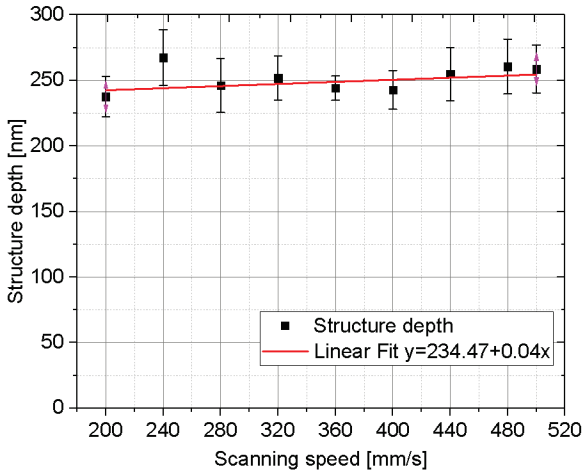


**Fig. 6** Diagram of structure depth vs varied scanning speed

### 3.4 Scale-up of the patterning speed for large area

Limited by the maximal travel and motion speed of linear working stage, a tool steel sample of 100 mm×100 mm area (shown in Fig. 7) was patterned with a structuring speed of 500 mm/s. The laser fluence applied was 1.85 J/cm$^2$. Spots distance was 175 μm, and two pulses per position. With these processing parameters, the 100×100 mm$^2$ area can be produced in approximately two minutes, demonstrating a high efficiency of this technique to fabricate periodic sub-micrometer structures.

Since the effects of diffraction on the patterns fabricated by MBI is dependent on the observation angle, as a result, periodic belts dazzle in different color can be seen in Fig. 7(a) and (b). Under an ordinary lateral white light illumination, the sample demonstrates a uniform diffractive effect over the whole length. This can be a result of well-defined line-like microstructures on the surface. The structural characteristic on the sub-micrometer structures investigated by AFM analysis are shown in Fig. 7(c)-(f). The average depth of the measured area is 251.98 nm and the periodicity is 934 nm. The aspect ratio of the microstructure is approximately 1:3.7. Fig. 7(e) shows the 2D FFT of the periodic structure in Fig. 7(c), the intensity of the peaks is extracted by drawing a line across the peaks and is shown in Fig. 7(f). A spectrum with 0$^{th}$ order and higher orders symmetrically distributed is depicted. The length between the ±1$^{st}$ order and 0$^{th}$ order is measured to be 1.07 μm$^{-1}$, which indicates the spatial frequency of the periodic structure in the frequency-domain and indirectly the periodicity of the microstructures. In this case, it is in excellent agreement of the measurement value 934 nm. The value of FWHM (full width at half maximum) of the ±1$^{st}$ order indicate the deviation of the periodicity. The smaller the FWHM value, the more homogenous is the periodic structures.

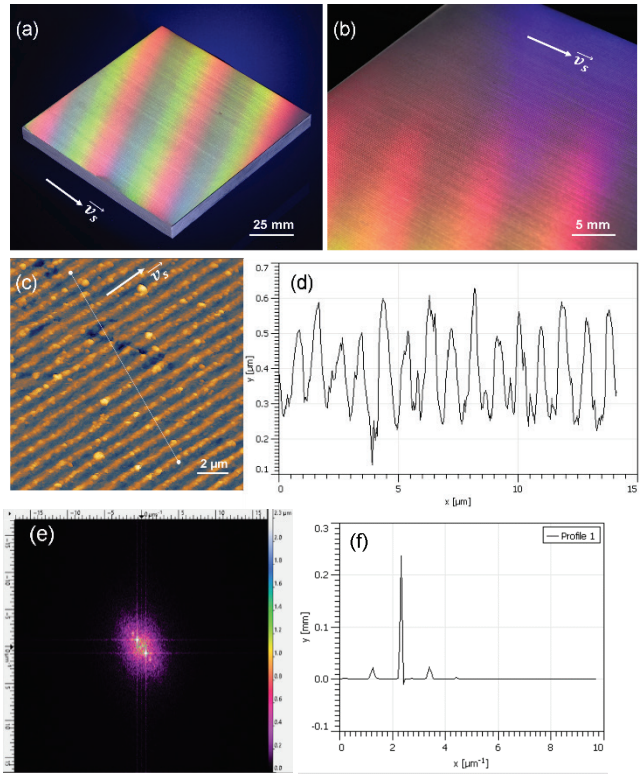


**Fig. 7** A large-scale tool steel sample 100 mm×100 mm patterned by multi-beam interference. (a) and (b) optical images of the diffractive effect on the patterned surface in different magnification, (c) AFM image of the line-like microstructure on the sample and (d) its profile, (e) and (f): 2D FFT analysis on the periodicity of patterned structures.

## 4. Conclusion

We demonstrated the possibility to enhance the patterning efficiency by stabilization the pulse energy deposition during the structuring with a speed of 500 mm/s. In this process, the positon synchronized output of the motion axis is utilized. The pulse overlap or pulse density, which is normally dependent on scanning speed and pulse repetition rate, has a determinative influence on the ablation results. With the function of position synchronized output system, the pulse position is fixed and independent on the structuring speed during the patterning process. Thus, the influence of speed variation is minimized and a homogeneous pattern with stable ablation depth and constant structural periodicity can be fabricated on a large-scale area.

The homogeneity of the large area patterning was characterized by structural and optical analysis. By means of an atomic force microscopy and a 2D FFT analysis, the profile of patterned structures can be precisely extracted and characterized. Stable structure depth and periodicity of microstructures patterned by varied speed give evidence to the feasibility of scaling up the structuring efficiency using PSO. As a final remark, by using a 532 nm wavelength ultrashort pulsed laser irradiation, we have achieved a structuring speed of 500 mm/s for a 100 $cm^2$ area on a well-polished tool steel, which corresponds a patterning speed of 60 $cm^2$/min. The efficiency of patterning with multi-beam interference can be further enhanced by employing a faster motion speed of axis.

**Acknowledgments**

The depicted research was funded by the Deutsche Forschungsgemeinschaft (DFG) as part of the program Cluster of Excellence "Integrative Production Technology for High-wage Countries" at RWTH Aachen University.

**References**

[1] G. M. Burrow and T. K. Gaylord: Micromachines, 2, (2011) 221.
[2] J. Berger, T. Roch, S. Correia, J. Eberhardt and A. Lasagni: Thin Solid Films, 612, (2016) 342.
[3] D. Guenther, , J. Valle, S. Burgui, C. Gil, C. Solano, A. Toledo-Arana, R. Helbig, C. Werner, I. Lasa, and A. F. Lasagni: International Society for Optics and Photonics X, 9736, (2016) 973611.
[4] L. Müller-Meskamp, Y.H. Kim, T. Roch, S. Hofmann, R. Scholz, S. Eckardt, K. Leo, and A. F. Lasagni: Adv. Mater., 24, (2012) 906.
[5]. M. Birnbaum: J. Appl. Phys., 36, (1965), 3688.
[6]. A. Borowiec and J. K. Haugen: Appl. Phys. Lett., 82, (2003).4462.
[7] E.L. Gurevich, and S.V. Gurevich: Appl. Surf. Sci., 302, (2014) 118.
[8] T.T. Dai Huynh, A. Petit, and N. Semmar: Appl. Surf. Sci., 302, (2014) 109.
[9] M. Huang, F. Zhao, Y. Cheng, N. Xu, and Z. Xu: Opt. Express, 16, (2008) 19354.
[10] R. Le Harzic, D. Dörr, D. Sauer, M Neumeier, M. Epple, H. Zimmermann and F. Stracke: Opt. letters, 36, (2011) 229.
[11] J. Schille, L. Schneider, M. Mueller, U. Loeschner, N. Goddard, P. Scully and H. Exner: J. Laser Micro/Nanoengin., 9, (2014) 161.
[12] J.P. Negel, A. Voss, M. Abdou Ahmed, D. Bauer, D. Sutter, A. Killi, and T. Graf: Opt. Lett., 38, (2013) 5442.
[13]. H. M. Phillips, D. L. Callahan, R. Sauerbrey, G. Szabó, and Z. Bor. Appl. Phys. Lett., 58, (1991) 2761.
[14]. P. Simon and J. Ihlemann: Appl. Phys. a-Materials Sci. Process, 63, (1996) 505.
[15]. Y. Nakata and N. Miyanaga: Appl. Phys. A Mater. Sci. Process, 98, (2010) 401.
[16] M. Bieda, E. Beyer, and A. F. Lasagni: J. Eng. Mater. Technol., 132, (2010) 031015.
[17] A. Lasagni, D. Benke, T. Kunze, M. Bieda, S. Eckhardt, T. Roch, D. Langheinrich and J. Berger: J. Laser Micro/Nanoengin., 10, (2015) 340
[18] V. Lang, T. Roch and A. Lasagni: Adv. Eng. Mater., 18, (2016) 1342.
[19] Florian Roessler and Andrés F. Lasagni. J. Laser Micro/Nanoengin., 13, (2018).68.
[20] M. Steger and A. Gillner: J. Laser Micro/Nanoengin., 11, (2016).296.
[21] C. He, M. Steger and A. Gillner: J. Laser Micro/Nanoengin., 13, (2018) 1.
[22] M. Steger, S. Boes, S. Thilker and A. Gillner: J. Laser Micro/Nanoengin., 9, (2014) 225.
[23] VDI 32540:2012-08. 2012, Beuth Verlag, Berlin.

(Received: June 27, 2018, Accepted: March 6, 2019)